Resonant Field Amplification and Rotational Screening in DIII-D RMP Simulations

V.A. Izzo, I. Joseph

Sherwood 2008

Boulder, CO

Motivation

- The impulse heat flux associated with large ELMs becomes unacceptably high for ITER
- The application of resonant magnetic perturbations (RMP) to DIII-D plasmas at low collisionality has achieved ELM suppression, primarily due to a pedestal density reduction
- The mechanism for the enhanced particle transport (without significantly enhanced heat transport) is unclear
- Stochastic transport theory applied to vacuum field calculations has not explained experimental observations
- NIMROD simulations allow both the calculation of the plasma response to the RMP fields, and the inclusion of additional transport due to macroscopic MHD motion

→ Clearly, other transport mechanisms associated with small scale turbulence are possible, but neglected in these simulations

Initial Conditions(1)

DIII-D shot 113317

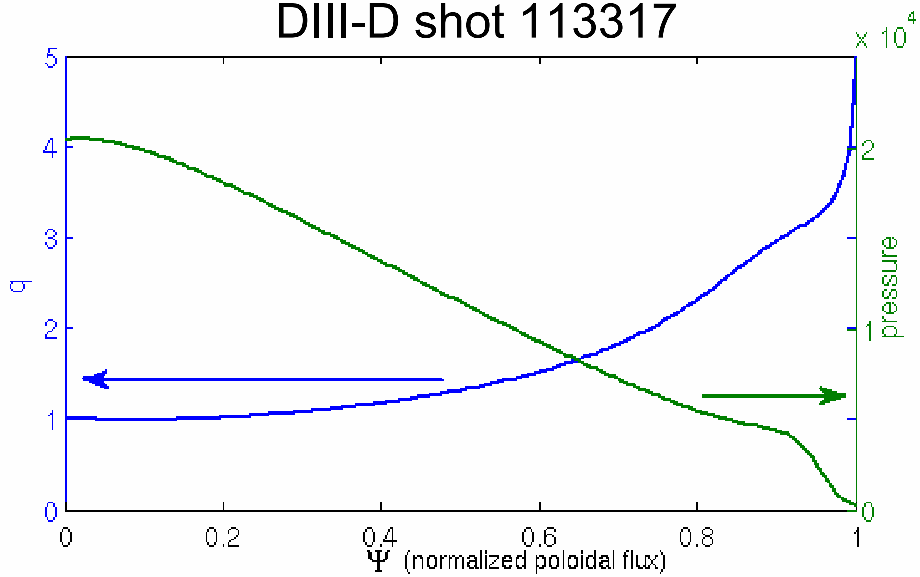

NIMROD grid

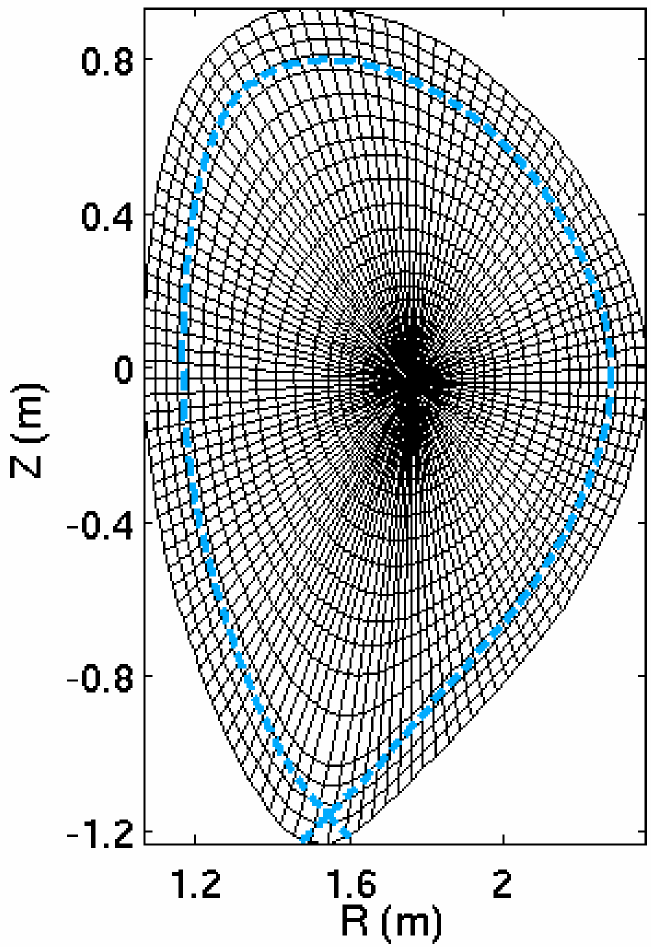

Grid: 20x120, w/ 5th order polynomials

Toroidal components n=0-5

Initial Conditions(2)

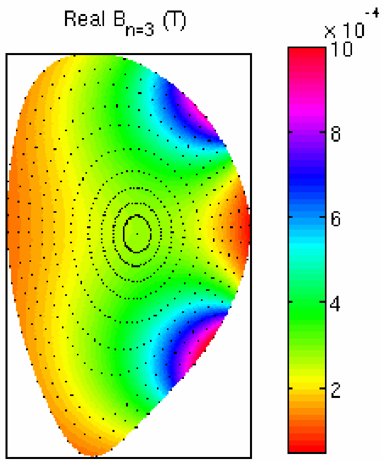

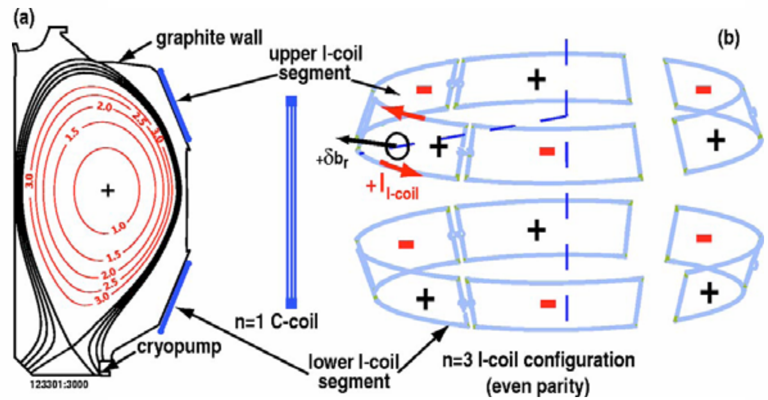

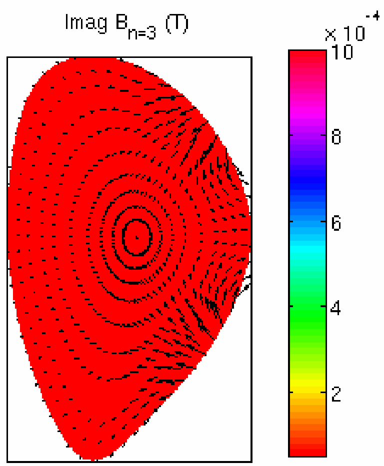

- Applied fields associated with DIII-D I-coils, C-Coils, and intrinsic error fields. (C-Coil fields are for error correction)
- Total perturbing field includes n=1,2,3 components, with n=3 being the largest

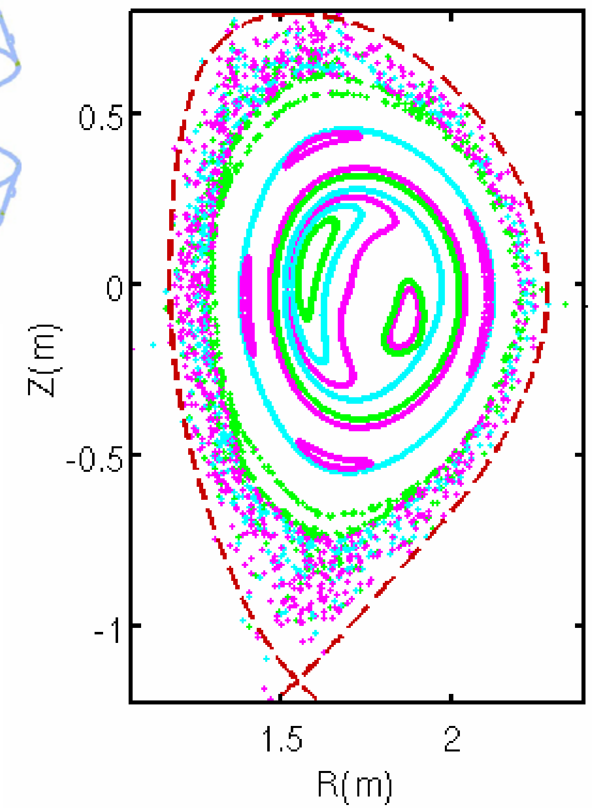

Initial Conditions(3)

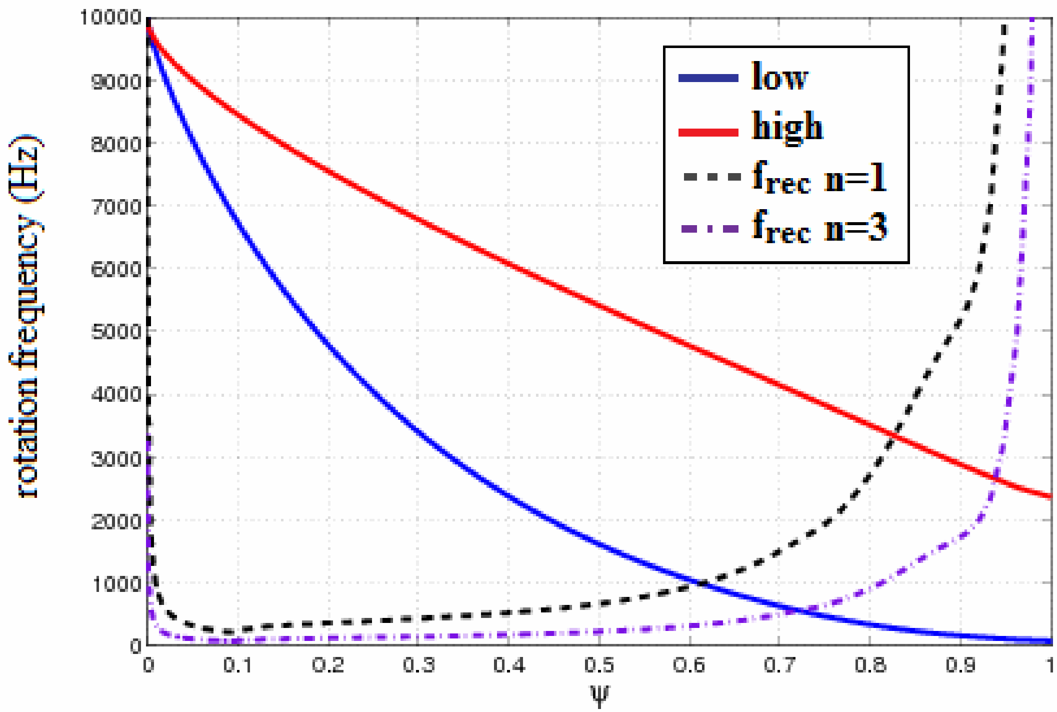

- Three rotation profiles simulated include no rotation, and two profiles shown at left with identical core values (110 km/s) but lower edge rotation in one case
- Rotation frequency is compared with reconnection frequency for n=1,3 modes at simulated parameters
- Simulation has resistivity enhanced 100 times above Spitzer value
- Simulation is in the visco-resistive regime

Less stochasticity with higher rotation

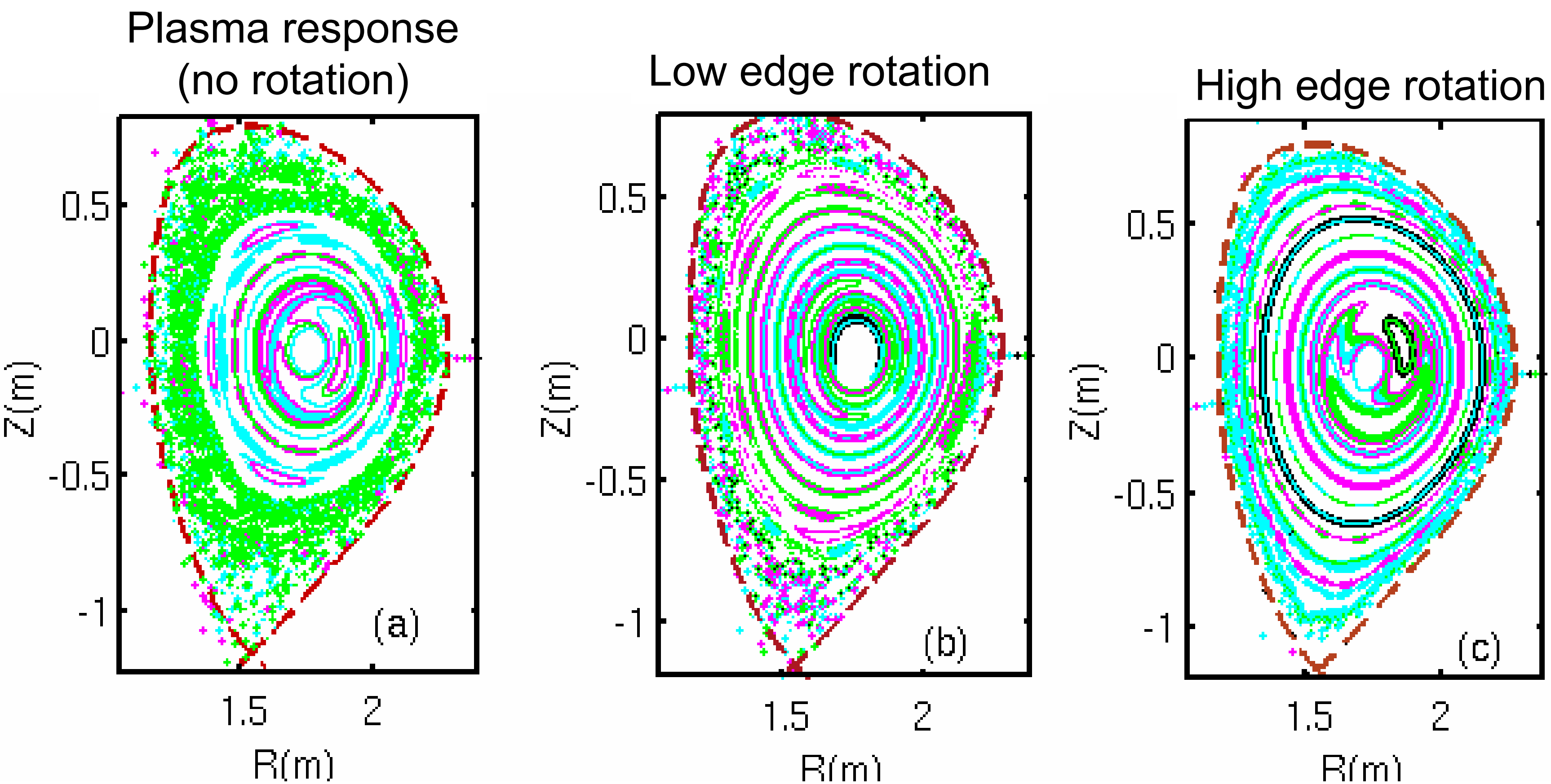

Plasma response amplifies resonant components of the field

Normal component of the n=3 B-fields (T)

White line on each plot is the resonant line m=-3q

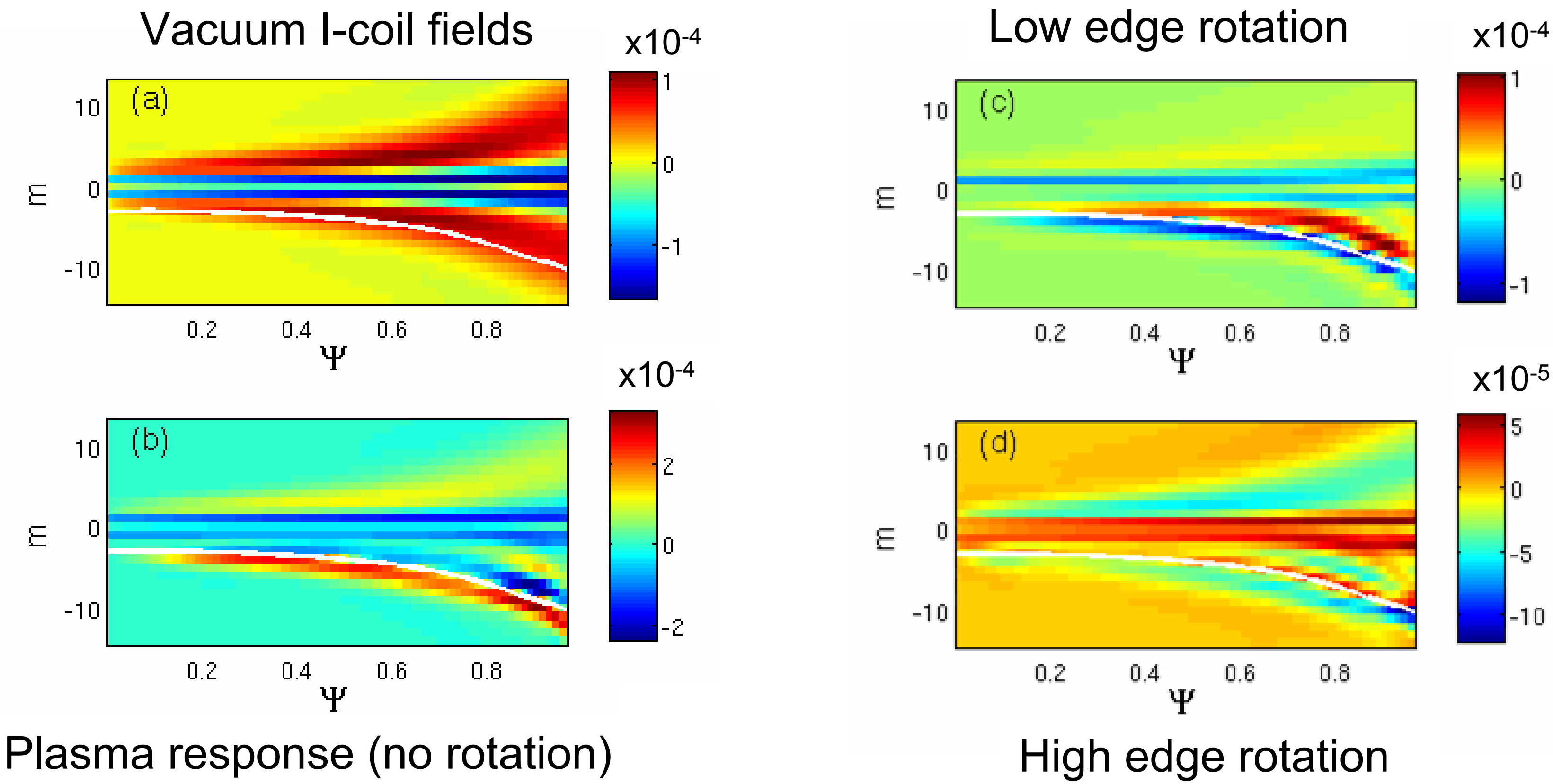

Without rotation, resonant components amplified by a factor of 2-5

- Amplitude and phase for each m are integrated over all Ψ
- Ratio of mode amplitude to vacuum I-coil mode amplitude
- All n=3 modes with m≤-4 are amplified for no rotation
- Amplification drops below unity for -6 ≤ m≤-4 with high edge rotation
- Nearly constant phase shift of π/5 for low edge rotation
- High rotation phase shift is not constant vs. m or in time

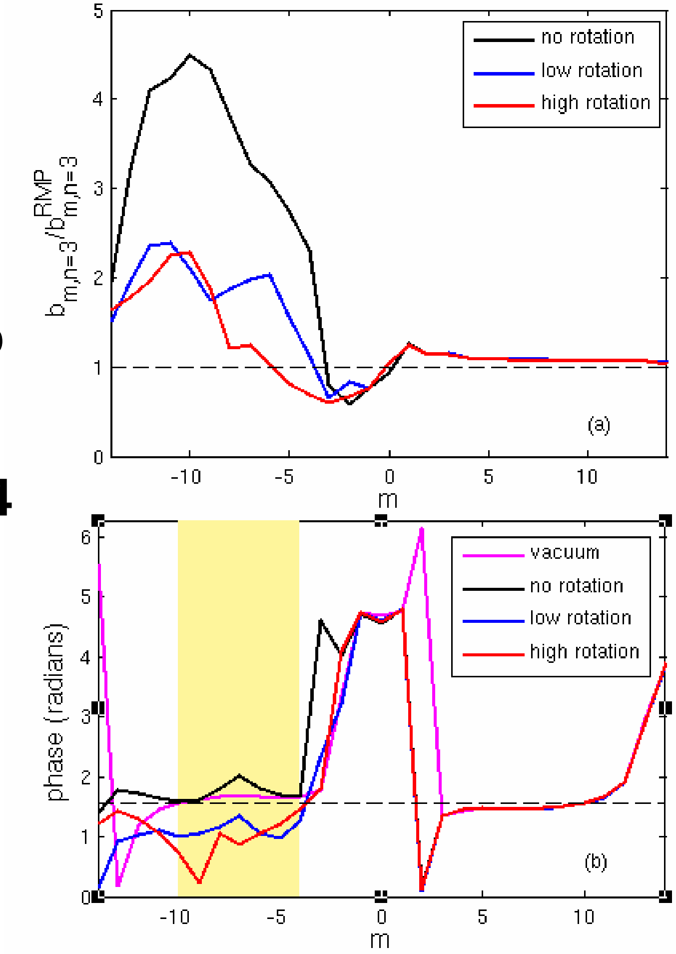

DIII-D NATIONAL FUSION FACILITY
UCSD

Rotation affects evolution of n=1, n=3 kinetic energy

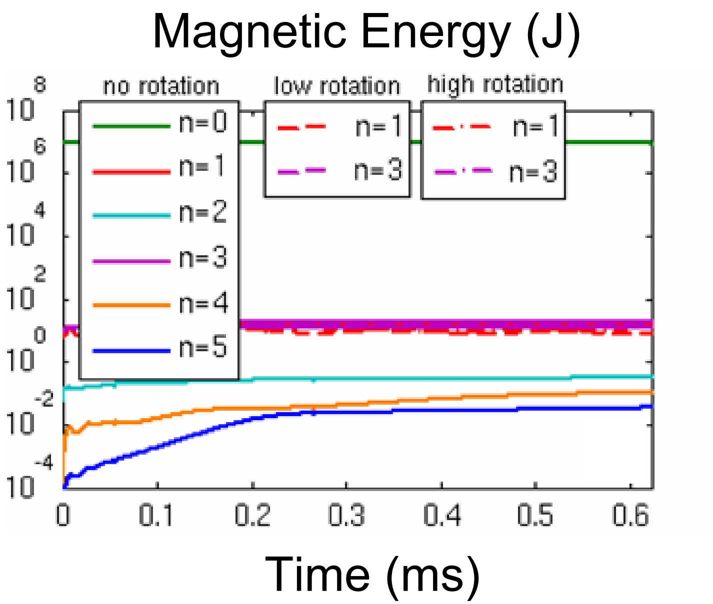

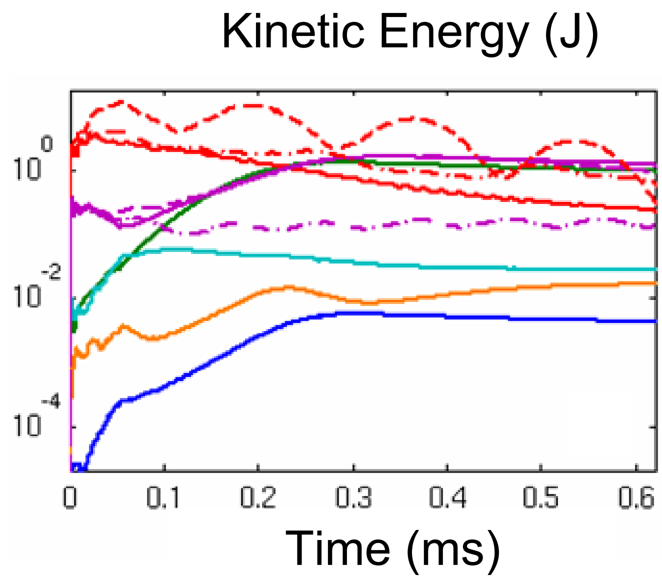

- n=3 flows are suppressed at high edge rotation
- 5.8kHz n=1 oscillation at low rotation, comparable to difference in q=1, q=2 rotation

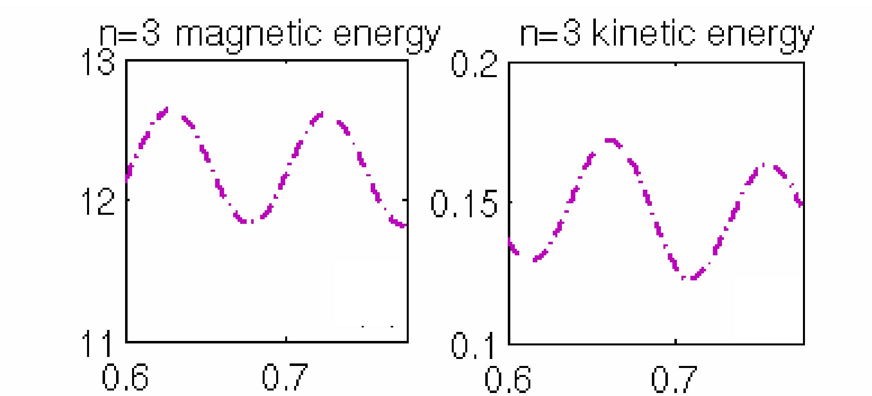

- (Left) n=3 energy on expanded scale for high rotation exhibits ~10kHz oscillation, equal to 3 times plasma rotation frequency at the edge
- Two energies oscillate 120° out of phase

Fitzpatrick* error field theory

Reconnected flux — Vacuum flux

$$\Psi_s = \frac{2m}{-\Delta' + \Delta(\omega)} \Psi_v$$

Tearing stability index

n times plasma rotation frequency

Boundary layer response to the applied error fields at the mode rational surface

→ Without rotation, error fields are amplified in tearing stable plasmas with $-\Delta' < 2m$

Visco-resistive regime

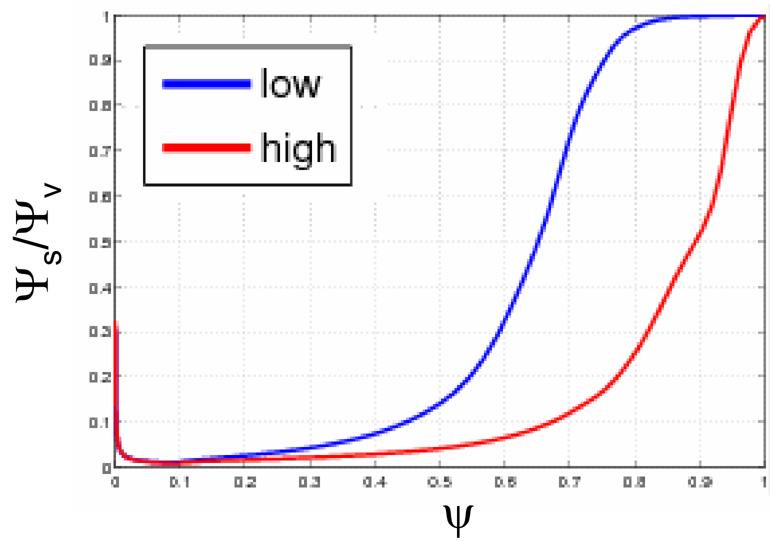

Screening factors calculated for the low and high rotation simulations assuming $-\Delta' = 2m$ (no amplification)

E×B convection across the separatrix reduces edge density

Poloidal Velocity **Density (no rotation)** **Density (high rotation)**

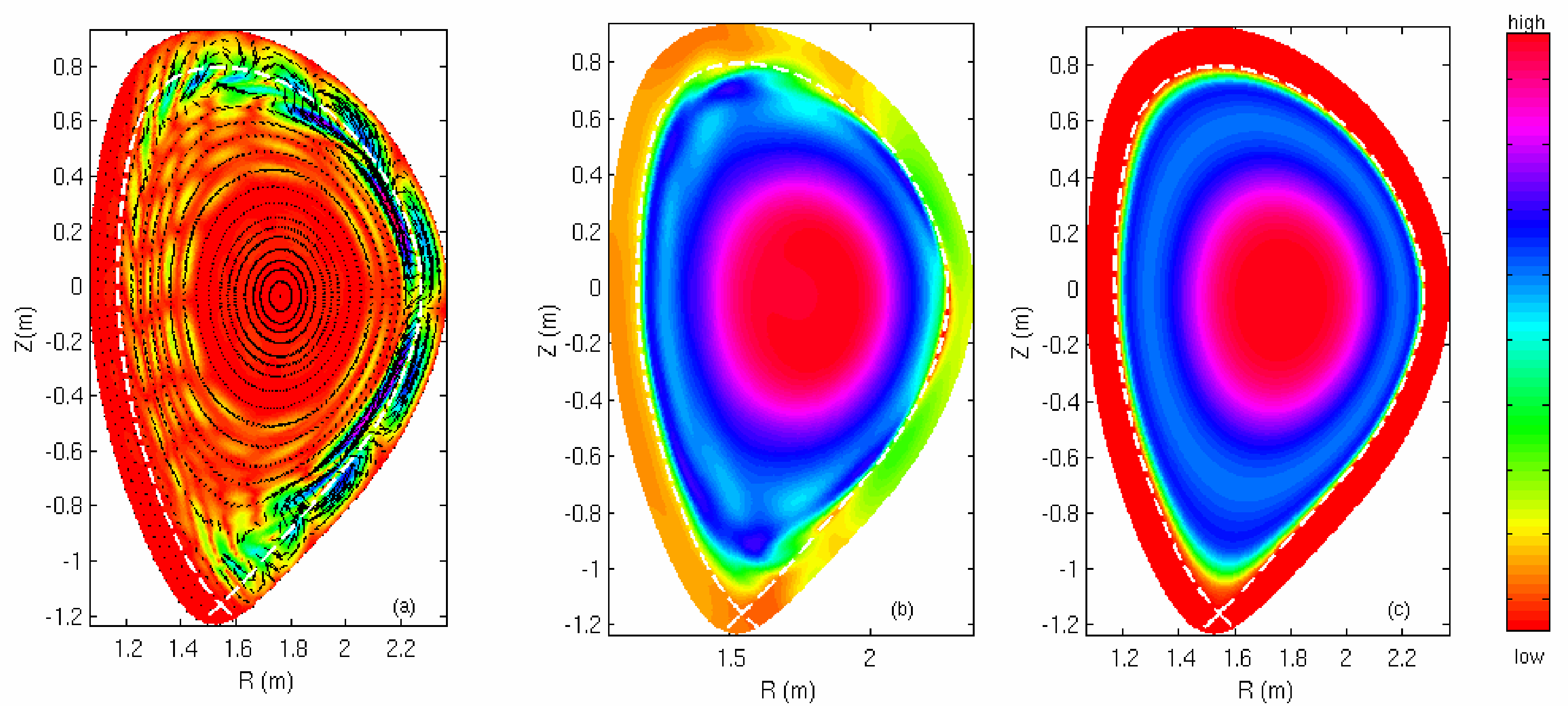

High edge rotation reduces E×B Motion, eliminates enhanced transport

Normal velocity along separatrix

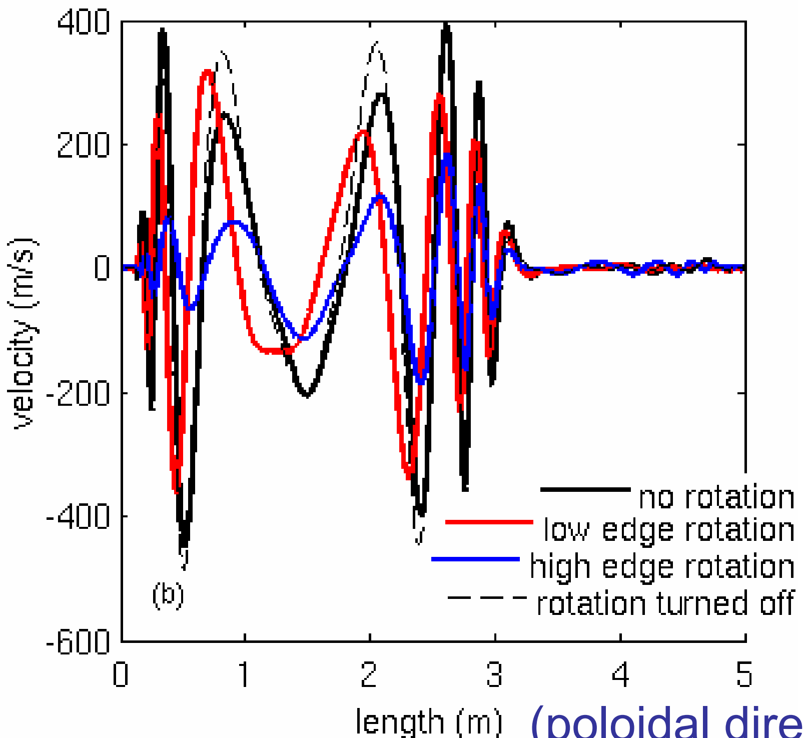

(poloidal direction)

x-point→outboard→inboard→x-point

Final Density Profiles

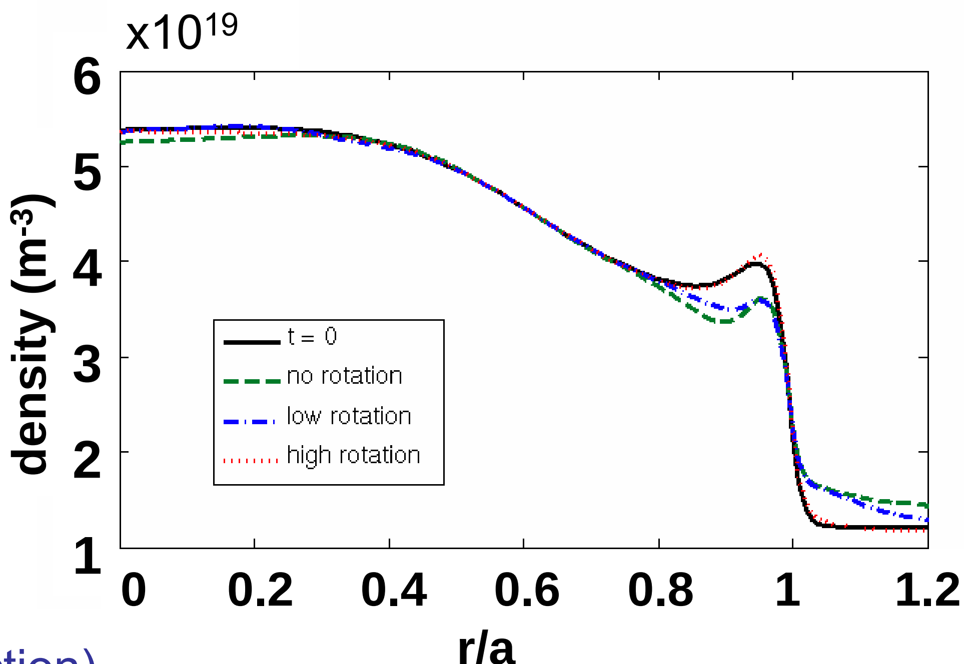

Temperature evolves similarly at high, no rotation

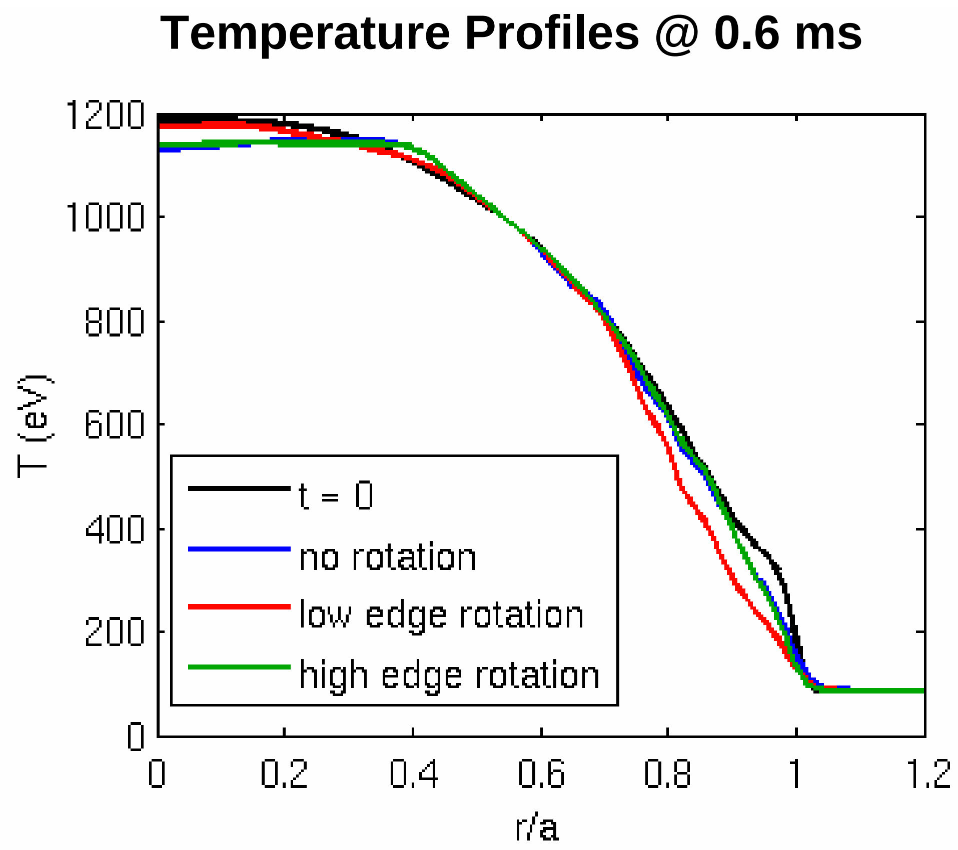

- Heat transport at the edge is enhanced in all cases, unlike DIII-D experiments
- Low rotation temperature profile differs from the other two, primarily due to smaller 1/1 mode in core (interaction between 1/1 and 2/1 mode)
- Overlay of high rotation and no rotation temperature profiles suggests particle transport and heat transport are not closely related

Transition from un-reconnected to reconnected state

Simulations begins at final state of high rotation case, but with the rotation turned off

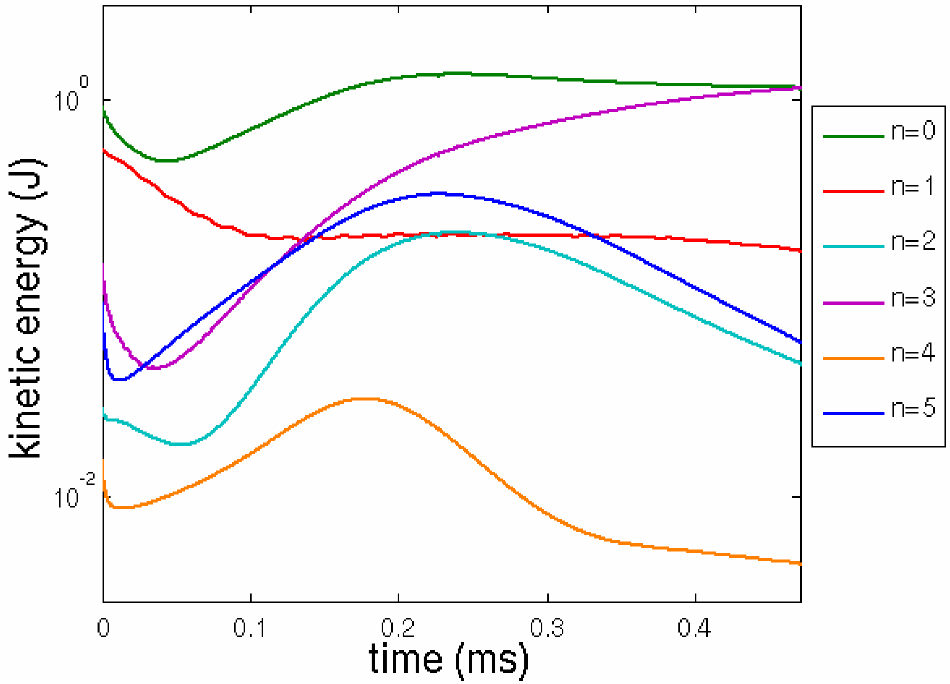

n=3 KE associated with E×B convection immediately grows

Magnetic fields again become stochastic throughout much of the volume

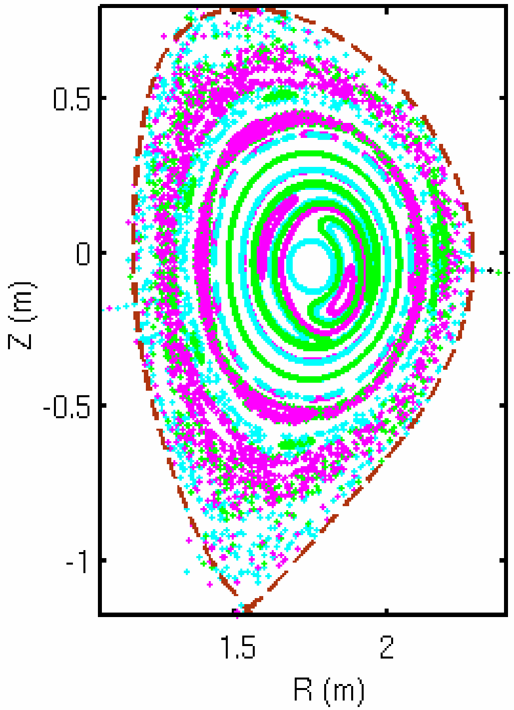

Density transport ensues as in previous non-rotating case

Heat and particle flux near the x-point

Surface for heat and particle flux plots

Locations corresponding to y-axis in plots on next 2 slides

(arbitrary units)

Simulation boundary

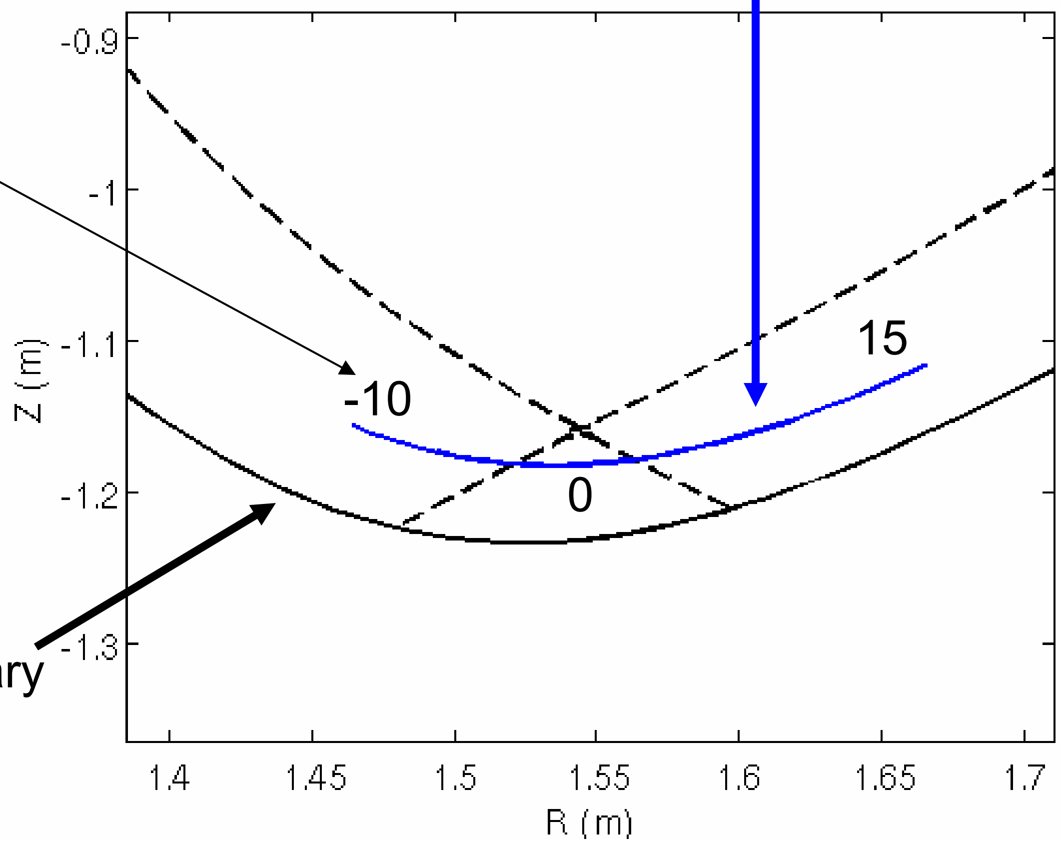

Heat flux near divertor is reduced by rotation

- Splitting of outer strike-point and n=3 structure is evident
- In both rotating cases, the peak heat flux is reduced by a factor of 2, as is the integrated heat flux over this region

→ How to reconcile with T profile similarities?

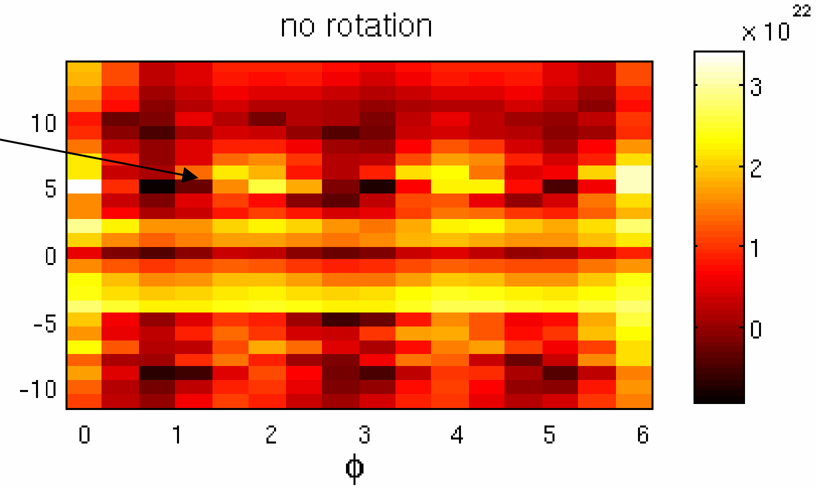

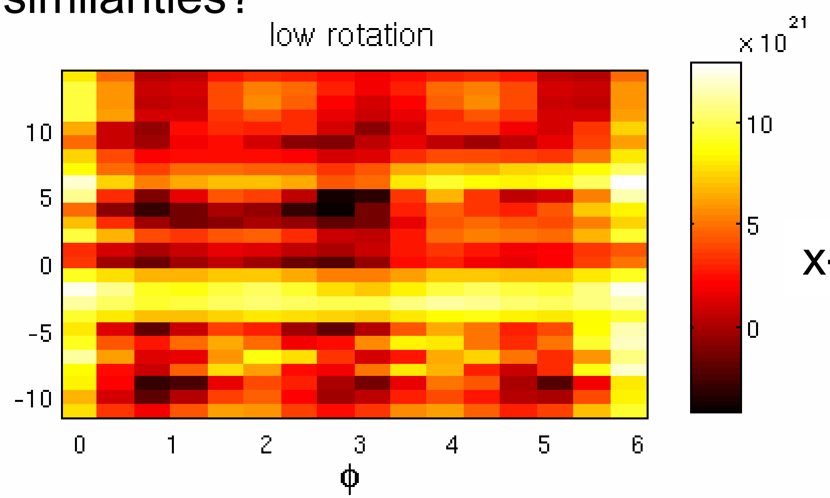

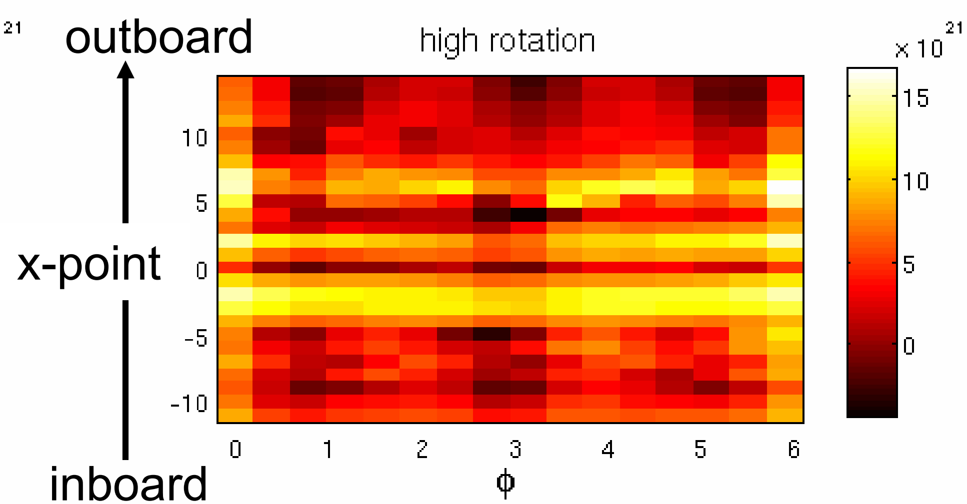

Rotation reduces n=3 variation of particle flux

• Strong n=3 variation in particle flux on outboard strike-point with no rotation

• n=3 variation is lessened with rotation, but amplitude increases on the inboard strike-point

• Positive is outward flux, negative is inward

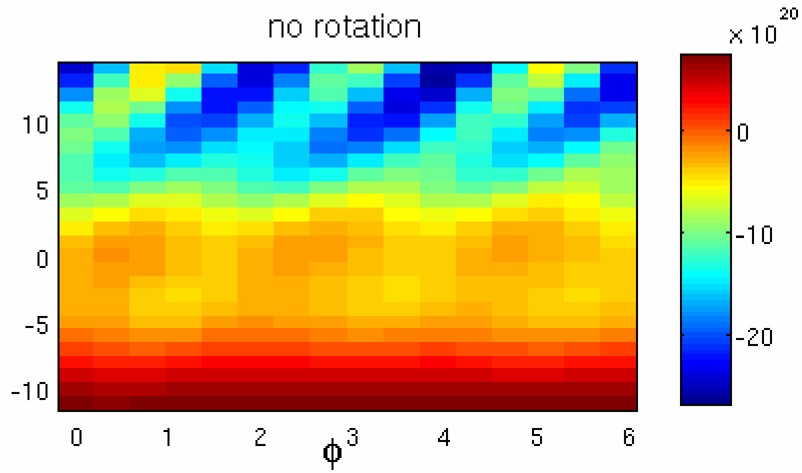

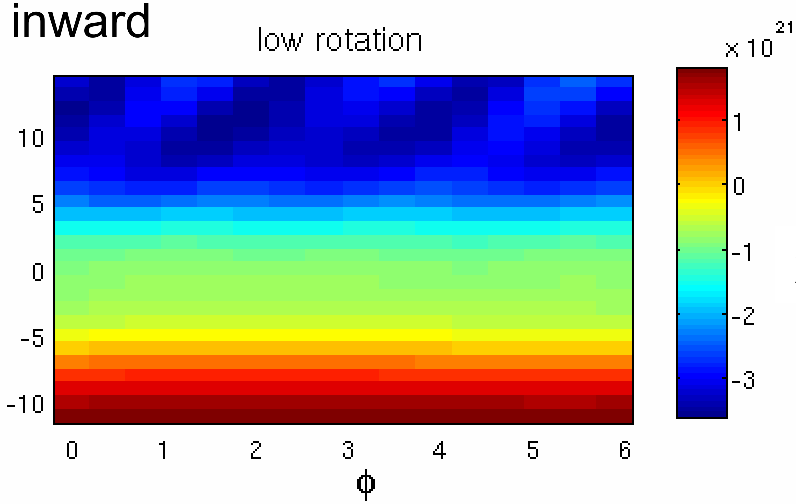

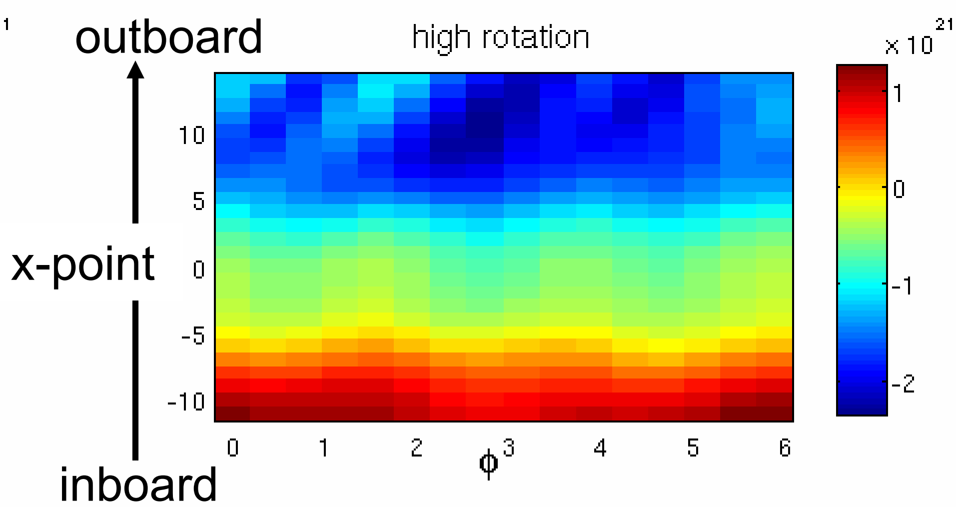

Conclusions

- Applied RMP fields in DIII-D NIMROD simulations are amplified by the ideal plasma response
- Rotational screening reduces resonant field amplitude, in some cases below the vacuum level
- Applied n=3 fields produce E$\times$B convection cells at the separatrix which enhance particle transport
- Sufficiently high rotation eliminates the enhanced particle transport
- Present NIMROD heat transport model gives pedestal temperature gradient reduction, in contrast with experiments

Future Work

- Scaling of rotation screening with plasma resistivity is most important factor to determine if E$\times$B mechanism is operative in real DIII-D plasmas
- Simulation of particular DIII-D RMP discharges with real rotation profiles, to make direct comparisons with data
- Modify the heat transport model to determine what model will reproduce the temperature pedestal gradient increase

The Rutherford Regime

In the non-linear "Rutherford" regime, Fitzpatrick* has the island width evolution equation:

$$W^2\left(\frac{dW}{dt}\right) = \frac{2mW_v{}^2 r_s}{0.8227\tau_R}\cos\omega t$$

Which he solves with the assumption W=0 when t=0 to get:

$$W(t) = W_0\left|\sin\omega t\right|^{1/3}$$

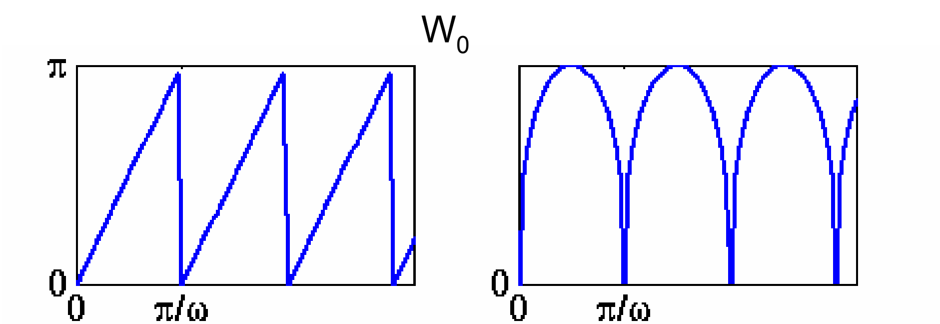

Fitzpatrick's solution has a frequency of 2ω (=2nΩ), whereas our n=3 oscillation has a frequency of ω.

But suppose we assume $W=W_v$ when t=0. Then we get:

$$W = (W_v{}^3 + W_0{}^3(\sin\omega t))^{1/3}$$

Provided $W_v > W_0$ (it is in our case for all $W_v > \sim 10^{-6}$m), we get $\phi=\omega t$ (no weird phase jumps) and:

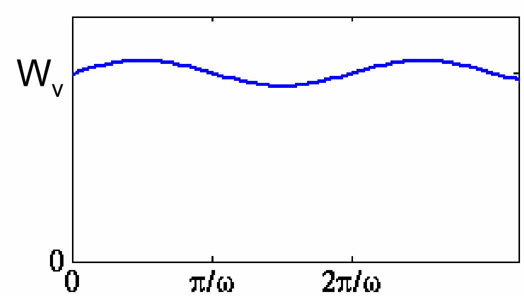

*Fitzpatrick, Phys. Plasmas **5** (1998) 3325.